

DRI File Copy

EDD ACCESSION LIST

DRI Call No. 84065

Copy No. 1 of 2 cys.

Project Report

TT-5

Frequency Scan Antenna Design for RPV Radar Sensors

F. G. Willwerth
J. A. Weiss

22 October 1975

Prepared for the Advanced Research Projects Agency
under Electronic Systems Division Contract F19628-76-C-0002 by

Lincoln Laboratory

MASSACHUSETTS INSTITUTE OF TECHNOLOGY

LEXINGTON, MASSACHUSETTS



Approved for public release; distribution unlimited.

ADA021898

The work reported in this document was performed at Lincoln Laboratory, a center for research operated by Massachusetts Institute of Technology. This work was sponsored by the Advanced Research Projects Agency of the Department of Defense under Air Force Contract F19628-76-C-0002 (ARPA Order 2752).

This report may be reproduced to satisfy needs of U.S. Government agencies.

The views and conclusions contained in this document are those of the contractor and should not be interpreted as necessarily representing the official policies, either expressed or implied, of the Defense Advanced Research Projects Agency of the United States Government.

This technical report has been reviewed and is approved for publication.

FOR THE COMMANDER

Eugene C. Raabe

Eugene C. Raabe, Lt. Col., USAF
Chief, ESD Lincoln Laboratory Project Office

MASSACHUSETTS INSTITUTE OF TECHNOLOGY
LINCOLN LABORATORY

FREQUENCY SCAN ANTENNA DESIGN
FOR RPV RADAR SENSORS

F. G. WILLWERTH
J. A. WEISS
Group 33

PROJECT REPORT TT-5

22 OCTOBER 1975

Approved for public release; distribution unlimited.

LEXINGTON

MASSACHUSETTS

ABSTRACT

A small program to explore the feasibility of a frequency-scanned antenna as a low-cost, light-weight answer to the requirements of the mini-RPV radar system for the HOWLS program resulted in construction and study of a slotted-waveguide laboratory embodiment of the device. A general formulation of the relationships connecting design parameters was carried out and employed for guidance in selection of waveguide size, band center, and slot spacing. A 30% band from 14.8 to 20.3 GHz in empty WR-42 waveguide was selected. The beamwidth, sidelobe level, gain, attenuation, and efficiency were studied, including the effectiveness of tapered illumination and the occurrence of spurious cross-polarized radiation, as functions of the frequency-controlled scan direction. Some thought was given to alternatives such as aperiodic-array and subarray techniques as means of reducing the tunable bandwidth requirement, as well as stripline serpentine-waveguide designs, for possible future investigation. The work reported herein has shown that the frequency-scanned antenna will provide a low-cost implementation practical for some system applications. If the limitation, primarily in instantaneous signal bandwidth are acceptable in the applications pursued, further investigation of alternate designs is recommended.

TABLE OF CONTENTS

	<u>Page</u>
ABSTRACT	iii
LIST OF ILLUSTRATIONS	vi
ACKNOWLEDGMENT	vii
I. INTRODUCTION	1
II. LINEAR ARRAY DESIGN	3
III. EXPERIMENTAL RESULTS	7
IV. ALTERNATE DESIGNS	9
V. CONCLUSIONS	12
APPENDIX - Design of Frequency Scan Arrays	20
REFERENCES	35

LIST OF ILLUSTRATIONS

<u>Figure</u>	<u>Page</u>
1. Aperture Illumination of 36 slot array at 15 GHz, 17.6 GHz, and 19 GHz.	13
2. Scan angle vs. frequency for 36 slot array.	14
3. Experimental 36 slot linear array.	15
4. Measured gain and sidelobe levels for 36 slot array.	16
5. Center frequency E plane pattern for 36 slot linear array.	17
6. Far-field antenna pattern of a slotted waveguide antenna. Waveguide WR-42; slot spacing $S = 0.406$ in; number of slots, $n = 256$. At frequency 17.547 GHz, the main lobe is pointed in the direction $\theta = -13.244^\circ$	18
7. Far-field antenna pattern of the slotted waveguide of the previous Figure, when the array of slots is divided into 16 subarrays of 16 slots each, and a phase shift of 57.296 degrees per subarray is introduced. The main lobe is now pointed in the direction $\theta = -12.276^\circ$ and subarray grating lobes have risen to about 15 db below the main lobe.	19
8. Frequency scanned antenna dispersion diagram.	27
9. Bandwidth and center frequency of -40° to 0° scan designs.	28
10. Bandwidth and center frequency of -20° to $+20^\circ$ scan designs.	29
11. Waveguide width and number of elements for -20° to $+20^\circ$ scan.	30
12. Aperture length vs. frequency for 4 mrad beamwidth.	31
13. Serpentine line.	32
14. Serpentine line $F = 2$ dispersion diagram.	33
15. Bandwidth and center frequency $F = 3$ serpentine line design -20° to $+20^\circ$ scan.	34

ACKNOWLEDGMENT

The authors are pleased to acknowledge the assistance of R. C. Aucoin and L. L. Mandeville in the fabrication and testing of the array.

I. INTRODUCTION

The objective of the joint ARPA/Army Hostile Weapons Locating (HOWLS) Program is to locate and identify hostile indirect fire weapons. One element of the program is to develop radar capabilities to detect, locate, and identify indirect fire weapons. In one possible application, such a radar would be installed in a mini-RPV (remotely piloted vehicle). A principal component for such a radar is a low-cost, light-weight antenna suitable for a mini-RPV. The requirement for an electronically scanned antenna was established during a radar design study. A phased-steered antenna was selected for an experimental system and proposed for an operational system because of its greater flexibility for the airborne radar task; however, the cost and weight of such an antenna represent a major part of the total radar in a mini-RPV application. It was felt that the inherent simplicity of a frequency-scanned antenna was sufficiently attractive to warrant an investigation of this approach. Although a frequency-scanned antenna is not suitable in applications which require signal bandwidths beyond about 25 MHz or which require frequency agility, there are applications where the lower cost and weight of the frequency-steered antenna would make it a cost effective approach. These include some form of both stand-off and investigator radars where the applicability will depend to a large extent on the target enhancement and identification techniques determined to be most effective.

A small effort was launched to investigate various ways of implementing a frequency-scanned array. The objective of this effort was to demonstrate the feasibility of scanning a 40° sector with a simple frequency-scanned antenna, and to determine the performance limitations of such an antenna.

The primary emphasis was the development of an antenna with 25 MHz instantaneous bandwidth and an 8 mrad beamwidth that has other performance characteristics comparable to the well-known narrowband frequency-scanned antennas as well as the simplicity, low-weight, and low cost features of such antennas. A literature search showed that slotted waveguide arrays had only been used for narrow tunable bands of about 10%, whereas, tunable bandwidths up to 30% may be required for the desired application. The most promising design candidate from the study was constructed, and its performance measured and compared with theoretical predictions.

II. LINEAR ARRAY DESIGN

The antenna design objectives were: beamwidth - 8 mrad, center frequency - 10-20 GHz; sidelobe level 20 db max; instantaneous bandwidth 25 MHz; scan range 40° azimuth; maximum loss 6db; tunable bandwidth 20%; scan volume to include broadside.

Because of their simplicity of fabrication, edge slots, slots cut in the side wall of a waveguide, were considered as the radiating element in this investigation. The radiation from an edge slot is polarized parallel to the long axis of the waveguide. In a linear array of edge slot radiators all inclined at the same angle from the vertical, broadside scan would occur when all slots are in phase. This would be at cutoff in the waveguide. The scan angle of this array is related to the feed waveguide by the relation $\sin \theta = \lambda/\lambda_g$, where θ is the angle from the normal to the array, λ_g is guide wavelength, and λ is free speed wavelength. This slot arrangement is not very desirable because of the cutoff condition for broadside and the rapid onset of grating lobes.

If one reversed the angle to the vertical of adjacent slots, this reversal introduces a 180° phase change between adjacent slots. The scan angle of this array is now related to the feed waveguide by the relation $\sin \theta = \lambda/\lambda_g - \lambda/2S$ where S is the element spacing. At cutoff the scan angle will be at a large negative angle; if $S = \lambda/2$ it would be -90°. As frequency is raised above cutoff the scan angle increases from -90° and will be broadside when $S = \lambda_g/2$. Because of the availability of broadside scan and the flexibility offered by the element spacing with respect to grating

lobes, the phase reversed slot design took preference over the nonreversed.

Design curves for linear arrays with phase reversed slots were generated for two scan conditions; $\pm 20^\circ$ azimuth scan and -40° to 0° azimuth scan. The design of linear frequency scanned arrays is addressed in greater detail in the Appendix. The ratio of the 8 mrad beamwidth to the 25 MHz instantaneous bandwidth together with the change in scan angle with change in λ determined the frequency of the low end of the band. A major disadvantage of the $\pm 20^\circ$ scan is that only dielectric filled waveguides can scan this volume without grating lobes occurring, as is shown in the appendix. Dielectric filled waveguide was judged unsuitable because of increased conductor loss and increased fabrication costs. Use of the -40° - 0° scan makes more use of the frequencies near cutoff and thus air waveguide designs are not limited by grating lobes as they are in the -20 to $+20^\circ$ scan. Conductor losses for air waveguide near cutoff are less than 1db/meter. A fine grain search was made for the air dielectric case and a design using standard waveguide (WR42) was found. The center frequency using the WR42 design is 17.54 GHz. The slot spacing S is .406". The tunable bandwidth for the 40° scan is 30%. Taking into account the beam broadening due to a tapered illumination the 8 mrad beamwidth can be accomplished with an aperture of slightly less than 3 meters.

Having chosen WR42 waveguide, slot conductances were measured over a 30% band for 1/16" wide slots inclined at a 20° angle to vertical for various depth of cut of the slot into the broad wall. The measurement technique used, was to measure the loss of a 20 slot section, subtract the

conductor loss, and assume that each slot contributed 1/20th of the loss. The individual conductance g is related⁽¹⁾ to the single slot attenuation $A(S)$ by $g = 1 - 10^{-\frac{A(S)}{10}}$.

At the center frequency, a 1/2 meter array was designed to have a 30 db Taylor illumination. Using the measured conductance versus frequency data, the Taylor illumination at the center frequency and the resulting illuminations at 15 GHz and 19.5 GHz were plotted and are shown in Figure 1. The slot conductance is maximum when the slot is resonant or a half wavelength long. At frequencies below the band center, the wavelength increases and the conductance of all the slots decreases uniformly. The illumination maintains Taylor shape with a decrease in efficiency.

At frequencies above the band center, the wavelength decreases. The slots on both sides of the center of the array approach resonant length and their conductance increases. The slots in the center of the array which were resonant at the center frequency are now longer than a half wavelength and their conductance decreases. This causes the illumination to deteriorate from Taylor to a double maxima shape as is shown on Figure 1. At frequencies slightly below 19.6 GHz, the reduction in the center conductances is equal to the increase in side conductances and the illumination is close to uniform.

Figure 2 shows the relation between scan angle and frequency. It should be noted that from 19.3 to 20.2 GHz, where the illumination has the double maxima shape, the scan range is from -3° to 0° .

The scan from -3° to 0° has an additional problem. As you approach broadside scan, the reflections from each slot begin to add in phase and will cause a large mismatch which is maximum at broadside where the phase is exactly 180° between slots.

Even though the predicted illumination shows that sidelobe levels will not be in spec at the high end of the band, it was decided to continue with the WR42 waveguide design because of the quick turnaround time in fabricating and testing the array with standard size waveguide, and the fact that only a small scan range, -3° - 0° , will be seriously affected.

III. EXPERIMENTAL RESULTS

The half meter slotted array (Fig. 3) was fabricated and tested over the 30% band. The VSWR was less than 1.2/1 from 14.8 GHz (low end of band) to 19.3 GHz. From 19.3 to 20.3 the VSWR increased to a maximum of 2.5/1. Maximum sidelobe levels averaged from band center to low end were 19db. From the center frequency to the high end, the sidelobe level increased so that at broadside the level was 11 db. Figure 4 shows the measured gain and sidelobe level over the frequency band.

The crossed polarized patterns showed that the array was forming another beam, as if the slots were not phase reversed, at a level of 6-10 db down from the main beam peak. This can be explained by the fact that a slot inclined to vertical by 20° , by geometric projection, will have a cross polarized component in the order of 6-10 db down and will not be phase reversed. Standard⁽²⁾ techniques of suppressing this mode are fitting a waveguide over each slot so that the unwanted mode is cut off, or forming a parallel plate waveguide with a polarized grating at the new aperture. Both of these approaches cause severe mismatch in the feed guide.

In order to avoid the mismatch, the extra complexity, and weight of waveguide sections or polarization gratings, a new technique was tried. A ($\epsilon' = 1.01$) urethane foam block was cut with a razor blade to have inserts spaced the same as the slots. The foam support with resistive card is then placed against the guide so that the resistive material is broadside to the waveguide and positioned between slots. The horizontal component from the slot is perpendicular to the resistive material and is not attenuated.

The unwanted perpendicular component is in the plane of the resistive card and is attenuated. Since the unwanted energy is attenuated and not reflected, there is no increase in the VSWR in the feed guide. At all frequencies the cross polarized level was reduced below the level of the first sidelobe. The copolarized pattern was not affected until the scan reached -30° , and at the band edge -40° there was a reduction in gain of 1 db. It must be remembered that the cutting and spacing of the inserts were done with a razor and ruler; an accurately fabricated suppressor would have even less effect. The foam layer over the slots also provides weather proofing.

The sidelobe level at the design center frequency was 20 db. Slot depth and spacings tolerance of $\pm .005''$ and waveguide bowing caused phase errors which resulted in increased sidelobe levels from those predicted from the conductance illumination data. Measured pointing angle and frequency data showed a maximum deviation of $1/2$ degree from predicted values. This is within the accuracy of the synchro position sending unit.

Gain measurements were made every 500 MHz and compared to theory to determine if the loss of the slot radiation would be intolerable. From these measurements and calculations, the loss of the waveguide and slots at all frequencies is less than 0.5 db. A center frequency pattern is shown in Fig. 5.

Small quantity production costs were estimated for a 3 meter edge slot array in quantities of 12 units. The cost, including set up charges would be \$300/Array. The weight would be 1.6 pounds.

IV. ALTERNATE DESIGNS

Alternate frequency scanned antenna designs have also been investigated in order to determine if the tunable bandwidth can be reduced or if attractive mechanical alternatives can be found. In order to have polarization flexibility, topwall slots which radiate vertical polarization were studied to determine conductance values and bandwidth.

The possibility of using a subarray arrangement of elements in a frequency-scanned array antenna was considered, to see whether the rather severe requirement on tunable bandwidth could be reduced. A simple example of a subarray design would be one in which a linear array of N elements is subdivided into r sections, with the i -th section embracing n_i elements; $(i=1 \text{ } \Sigma \text{ } r)n_i = N$. The subarrays would receive excitation from a single source through the outputs of a power divider, with introduction of an appropriate phase shift into each subarray channel. Alternatively, suitably phased subsources could be used. The objective is to achieve an optimum combination of beamwidth, sidelobe suppression, and frequency-tunability over the required scan angle.

Such an arrangement cannot give an improvement by way of reducing the tunable bandwidth, at least in the simplest, most regular special case in which the subarrays are of equal length and composed of equal numbers of radiating elements. Briefly, the reason for this is that the scan direction angle θ depends solely on the waveguide propagation parameter $x = -1 + k_g s / \pi$, where k_g is the guide propagation constant and s is the element spacing. Attempts to simulate the condition of scan angle θ by means of irregular

spacing or excitation of elements, or by division of the array into non-uniform subarrays, tend to introduce θ -dependent irregularities in the far field phase front, creating intolerable sidelobes. An illustration of this situation for the case of a 256-element array divided into 16 equal subarrays is shown in Figures 6 and 7. Fig. 6 shows the far-field pattern for a uniformly illuminated linear waveguide array of the type described above. The parameters of the design are given in the Figure caption. Fig. 7 shows the effect of dividing the 256-element array into 16 subarrays of 16 elements each and introducing a phase shift of 57.296° per subarray (equivalent to 3.581° per element) into the subarray feed lines. The main lobe has turned 0.968° , from -13.244° to -12.276° , while the grating lobes corresponding to the spacing of the subarrays have risen to about 15 db below the main lobe.

The consideration of non-uniform or aperiodic styles of geometry or of excitation brings to mind, however, work which has appeared in the literature⁽³⁻⁷⁾ from time to time on the design of aperiodic arrays so arranged as to achieve precisely the opposite effect; namely, the suppression of sidelobes. The present survey does not exclude the possibility that an acceptable trade-off may exist in the design of an aperiodic frequency scanned subarray design which reconciles the requirements of beamwidth, sidelobe level, and tunable and instantaneous bandwidth. It does suggest that a rather sophisticated wave-theoretical study would be required; work reported in the literature up to the present time has yielded results of uncertain value and uncertain design procedures, even in the relatively

simpler case of scanning by variable phase-shifters, as contrasted with our present objective of frequency-scanning.

Investigations into serpentine lines shows the most promise of reducing bandwidth (Appendix 1). An air stripline design Δ_g , which meets the design objectives, with a serpent ratio of 3 (the length of the conductor is three times the element spacing) had a tunable bandwidth of 19.3% and a loss of less than 3db. The printed circuit approach also makes it economically feasible to match each slot radiator and scan through broadside with no gain reduction.

V. CONCLUSIONS

The objective of scanning a 40° sector with a frequency-scanned array which has the requirement of 25 MHz instantaneous bandwidth has been demonstrated. An analysis and design procedure for frequency-scanned arrays was developed and predictions using the analysis were verified with the experimental slotted array. Departure from predicted results in the sidelobe levels was caused primarily by the bowing of the waveguide. This could be eliminated by securing the array to a stiff plate before cutting the slots.

The major technical problem is the inclusion of broadside in the scan volume. The high VSWR at and about broadside could be reduced by matching every radiator. In a waveguide design, the matching network for edge slots would be capacitive screws in the top wall at each slot. This would add several additional steps in the fabrication process and would impact severely on the cost. In a printed circuit antenna, such as the serpentine line design with a 19% tunable bandwidth, each slot radiator could be matched with no increase in fabrication costs.

A waveguide design for a 40° scan from -45° to -5° can be accomplished in a 25% tunable bandwidth. The reduction in bandwidth, and avoidance of broadside scan would result in more control of the aperture illumination, and a low VSWR throughout the band.

Future effort should be devoted to investigating printed radiators. The radiator should have small conductance values required in a large array, and be adaptable to a traveling wave antenna with 20% bandwidth.

With such a radiator, a serpentine line design can be fully implemented.

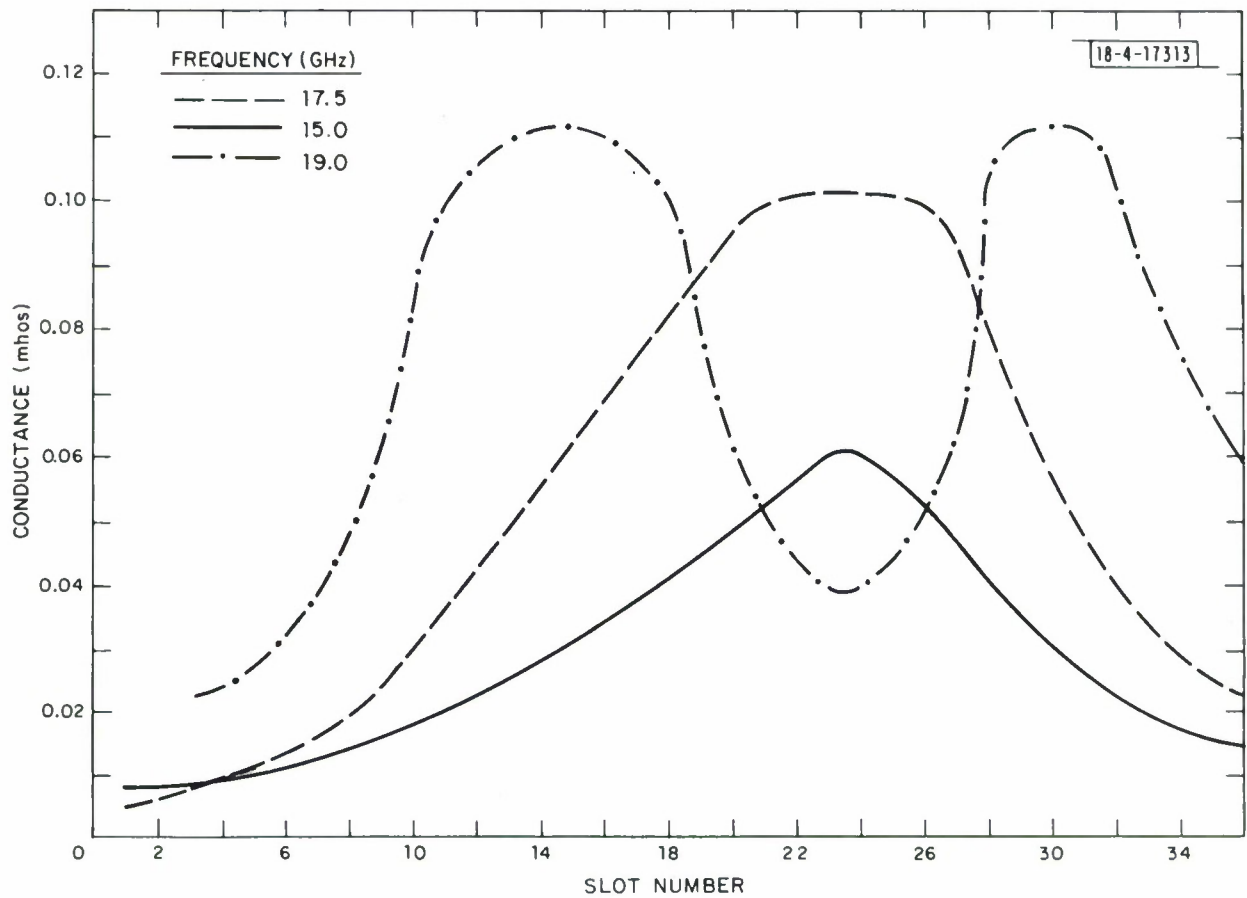


Fig. 1. Aperture Illumination of 36 slot array at 15 GHz, 17.6 GHz and 19 GHz.

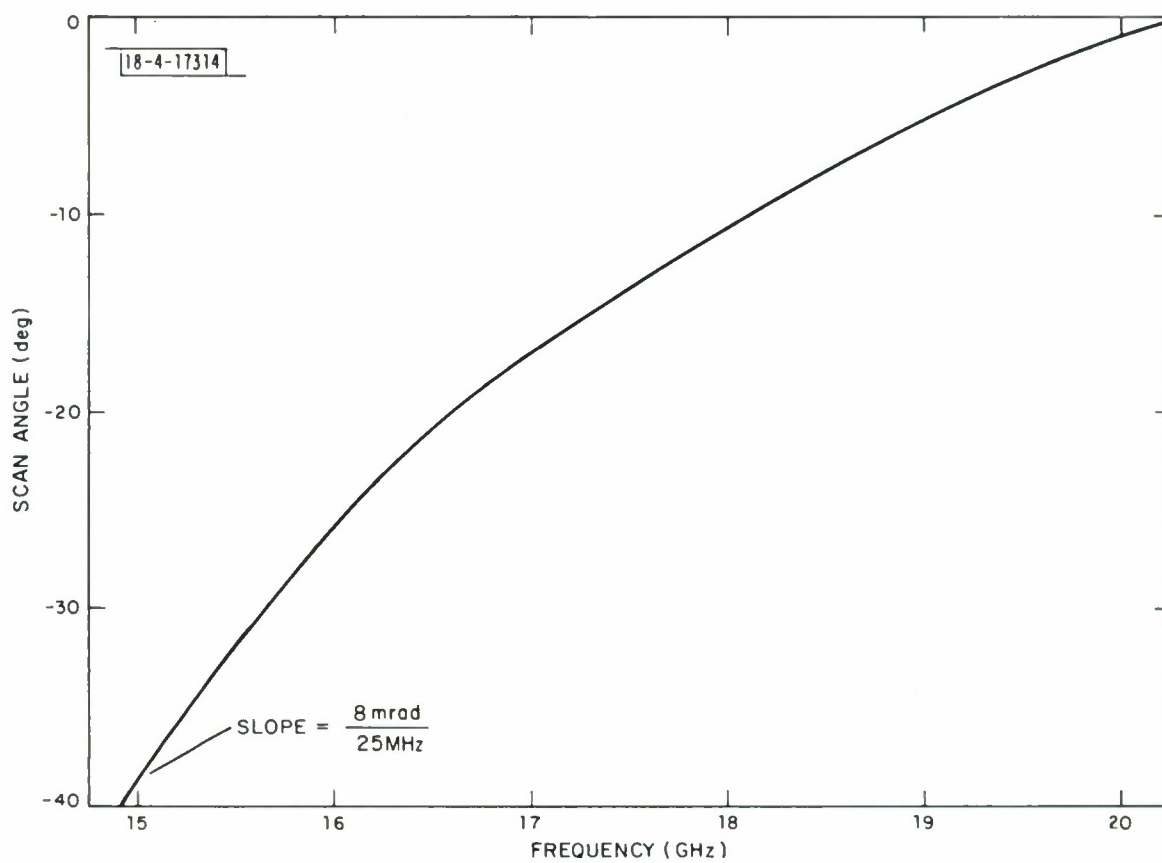


Fig. 2. Scan angle vs. frequency for 36 slot array.

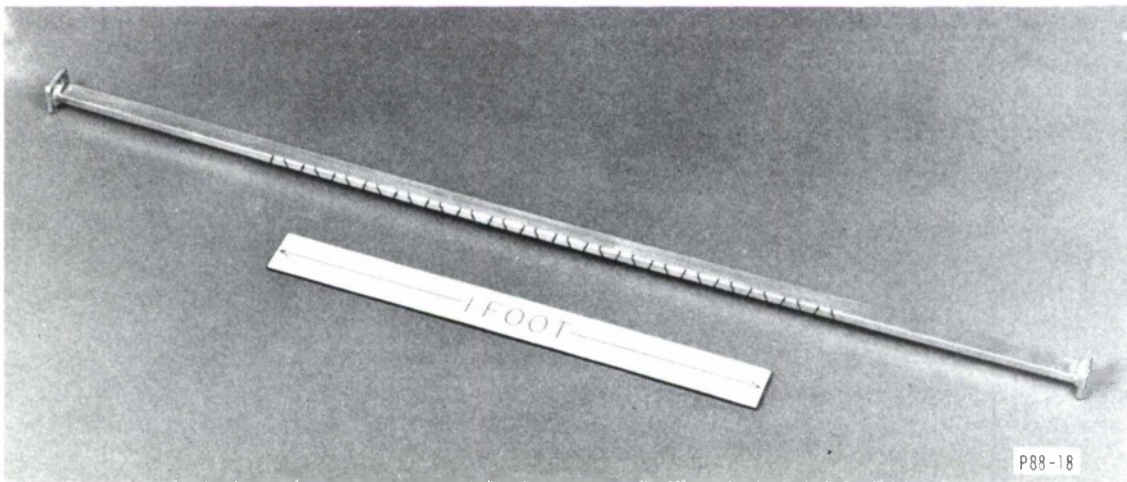


Fig. 3. Experimental 36 slot linear array.

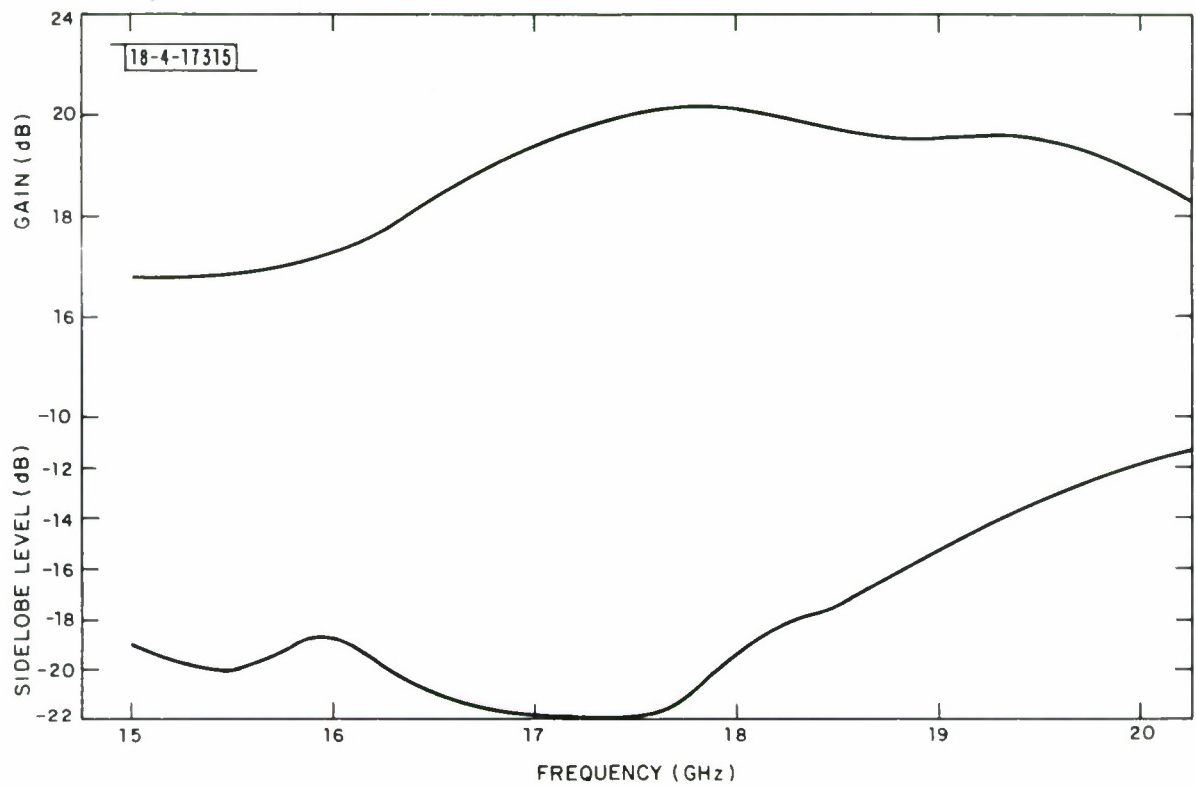


Fig. 4. Measured gain and sidelobe levels for 36 slot array.

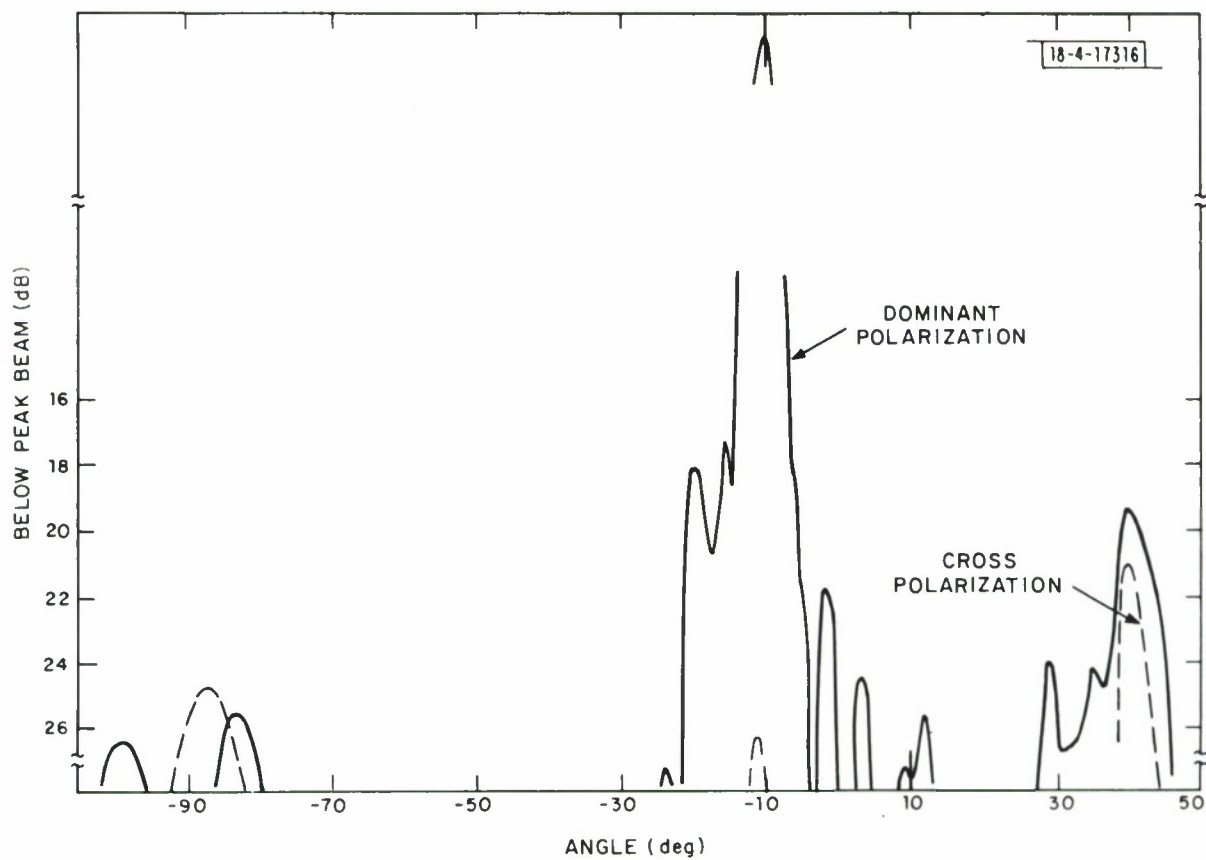


Fig. 5. Center frequency E plane pattern for 36 slot linear array.

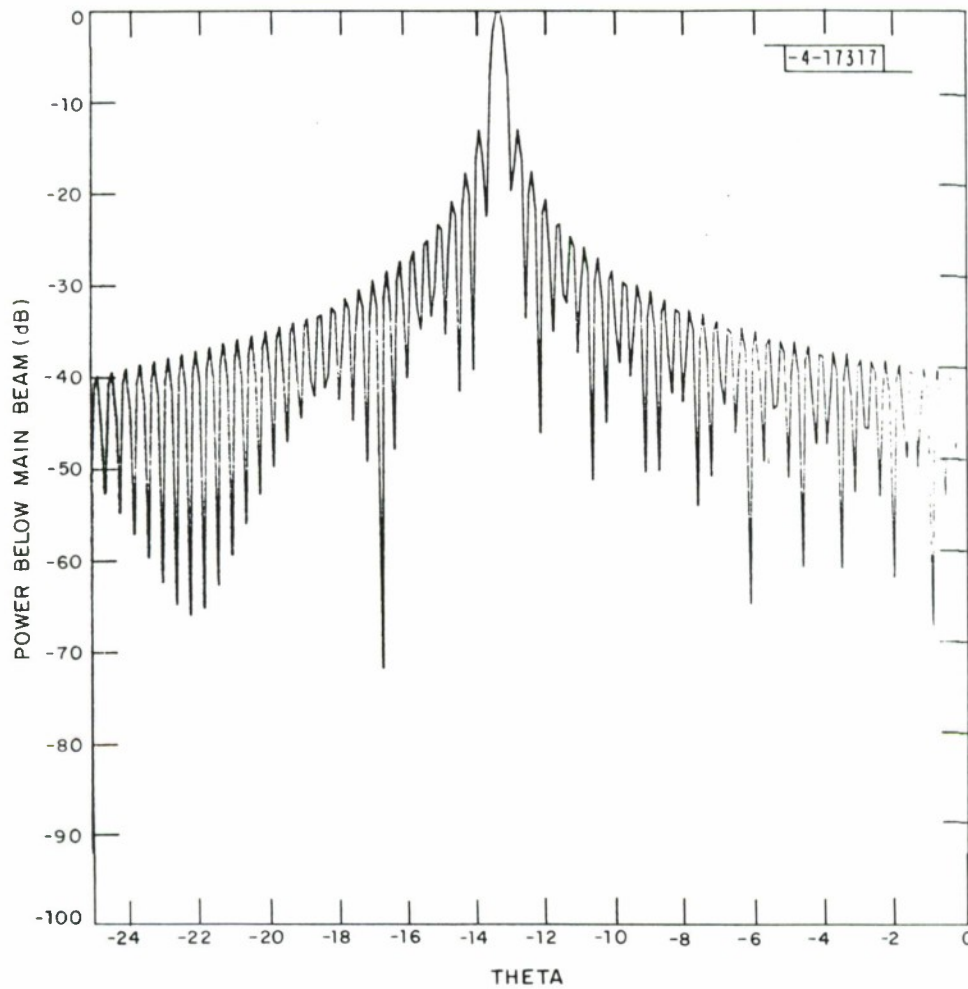


Fig. 6. Far-field antenna pattern of a slotted waveguide antenna. Waveguide WR-42; slot spacing $S = 0.406$ in; number of slots, $n = 256$. At frequency 17.547 GHz, the main lobe is pointed in the direction $\theta = 13.244^\circ$.

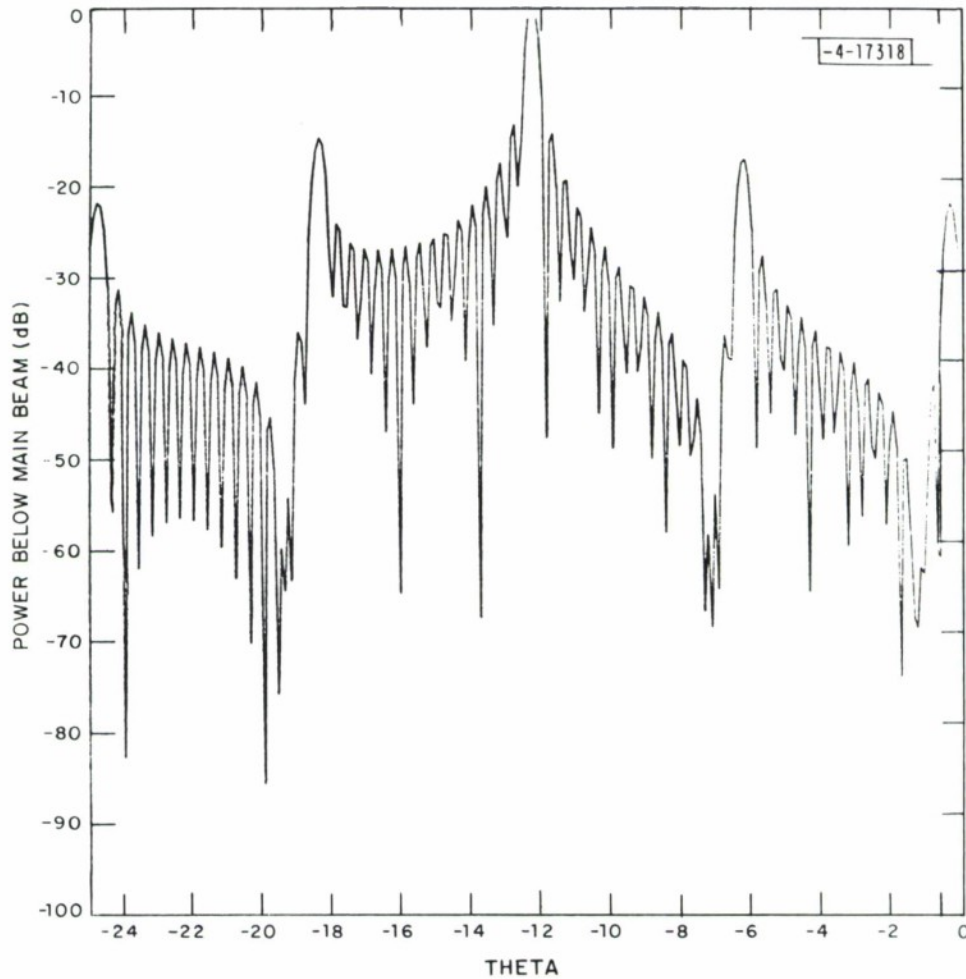


Fig. 7. Far-field antenna pattern of the slotted waveguide of the previous Figure, when the array of slots is divided into 16 subarrays of 16 slots each, and a phase shift of 57.296 degrees per subarray is introduced. The main lobe is now pointed in the direction $\theta = -12.276^\circ$ and subarray grating lobes have risen to about 15 db below the main lobe.

APPENDIX

Design of Frequency-Scanned Arrays

In this Appendix we summarize the logical flow of the design analysis of a frequency-scanned waveguide array antenna. The objective is to satisfy a combination of system specifications on angular beamwidth and instantaneous bandwidth, originating from the width and range interval of the illuminated area, without incurring excesses in tunable bandwidth, power dissipation, or design complexity. Thus, from tentative specifications of signal-to-clutter ratio of 10dB for targets of area 15 dBSM in terrain of reflectivity -10dB viewed in a slant direction from an aircraft flying at about 1 km altitude, we look for a main beam angular width of 4 mrad and range-gate capability corresponding to instantaneous bandwidth of 25 MHz. To avoid excessive diffusion of the beam on account of this bandwidth, the dispersion of the waveguide must be limited accordingly:

$$\frac{d\theta}{dv} = \frac{4\text{mrad}}{25 \text{ MHz}} = 1.6 \times 10^{-10} \text{ rad Hz}^{-1} \quad (1)$$

The structure envisioned is a simple, straight section of rectangular waveguide, which may be dielectric-filled, slotted at regular intervals in the alternately-phase-reversed style.

The dispersive characteristics of the waveguide, together with the above scan-rate specification, determine the minimum low-frequency end of the tunable bandwidth. We consider the dominant TE_{10} mode of rectangular waveguide, whose dispersion relation may be written

$$Ky^2 + (x+1)^2 = \left(\frac{s}{a}\right)^2 \quad (2)$$

in which K is the relative dielectric constant of the medium filling the waveguide; the parameters x and y represent the guide and space propagation constants, respectively:

$$x = -1 + \frac{k_g s}{\pi}, \quad y = \frac{k_o s}{\pi} \quad (3)$$

a is the guide width and s is the spacing of the radiating slots. For the variable x , the displacement by -1 from $k_g s/\pi$ incorporates the effect of alternate phase reversal of the radiating elements. For example, $x = 0$, corresponding to broadside beam direction $\theta = 0$, occurs for $k_g s = \pi$. The direction (scan angle) θ of the beam is given by

$$\frac{x}{y} = \sin\theta \quad (4)$$

The frequency-rate of scan $d\theta/d\nu$, always maximum at the low-frequency end of the tunable band, dictates the low-frequency limit ν_{\min} at scan angle θ_{\min} according to

$$\nu_{\min} = \left. \frac{y(d\theta/dy)}{d\theta/d\nu} \right]_{\theta_{\min}} \quad (5)$$

in which the factor $y(d\theta/dy)$ is determined from equations (2) and (4) to be

$$y \frac{d\theta}{dy} = \frac{1}{\cos\theta} \left(\frac{K}{\sin\theta + 1/y} - \sin\theta \right) \quad (6)$$

As for the high-frequency end ν_{\max} of the tunable band, we require that ν_{\max} fall below the frequencies of onset of both types of higher order modes: waveguide modes and spatial grating lobes.

From inspection of Fig. 8, one can draw a conclusion which was cited in Sec. II; namely, that the scan angle range from -20° to $+20^\circ$ can only be accomplished with guide containing a dielectric of $K > 1$. For empty guide, the dispersion curve runs into the grating lobe region slightly below the upper limit of $+20^\circ$. To see this, note that the asymptote of the dispersion curve, whose slope of $1/\sqrt{K}$ is equal to 1 in that case, intersects the grating lobe line at the point $(x,y) = (0.5, 1.5)$. The boundary line $x/y = \sin(+20^\circ)$ intersects that line at $(x,y) = (0.51, 1.49)$; slightly below, but nearly coincident with the intersection point of the asymptote. Thus, irrespective of the value of s/a which determines the spacing of the dispersion curve above its asymptote, the curve must cross into the grating lobe region at a scan angle less than $+20^\circ$. The closest approach to $+20^\circ$ would occur in the case $s/a = 0$, appropriate for TEM transmission lines such as stripline, which for $K=1$ results in a maximum scan angle of $\sin^{-1} (0.5/1.5) = 19.47^\circ$. For rectangular waveguides, the value of the maximum scan angle would be still smaller.

The foregoing design relations may be represented graphically with the aid of the waveguide dispersion diagram illustrated in Fig. 8, which presents the example for which $K = 4$ and $s/a = 1.5$. The vertex at $x = -1$ represents waveguide cutoff for the dominant mode, $k_g = 0$, which occurs for $k_o = k_c$ according to

$$k_c \sqrt{K} = \frac{\pi}{a}, \text{ or } y_c = \frac{1}{\sqrt{K}} \frac{s}{a}. \quad (7)$$

With increasing frequency, the curve approaches an asymptote whose slope is given by

$$\frac{dk_g}{dk_0} = \sqrt{K}, \text{ or } \frac{dy}{dx} = \frac{1}{\sqrt{K}} \quad (8)$$

The intersection with the line $y = 2-x$ represents the onset of the first spurious grating lobe, while the intersection with the lines $y = \pm x$ represent the extremes $\theta = \pm 90^\circ$ of the main beam scan angle. The tunable bandwidth is represented by the interval of the y-axis corresponding to the intersection of the dispersion curve with the lines indicating the scan-angle range called for by the system (illustrated in Fig. 8 for the case $\theta_{\min} = -20^\circ$, $\theta_{\max} = +20^\circ$).

We distinguish two styles of scan: symmetrically in the range between $\pm\theta_{\max}$, as illustrated in Fig. 8, and unsymmetrically over the range from the backward angle θ_{\min} to $\theta = 0$. Although the ability to scan through the broadside direction $\theta = 0$ has certain possible system advantages, it involves a difficulty in that at $\theta = 0$ there occurs a "Bragg reflection", or "stop-band", condition resulting in severe mismatch problems. To avoid this, we may confine the scan angle to backward (negative θ) directions with θ_{\max} designed to be at a small negative angle, about -5° .

The design analysis may be illustrated for a scan angle range of -40° to 0° . For minimum relative tunable bandwidth we wish to choose a dispersion curve for which cutoff occurs close to the low-frequency limit yielding $\theta_{\min} = -40^\circ$, but not so close as to exceed the frequency-rate of scan specification, eq. (1). To obtain a map of compatible parameters, we set up an array of points on a plane whose coordinates are s/a and K , as shown in Fig. 9. The coordinates s/a and K at a selected point on this plan, together with

$u = x_{\min}/y_{\min} = \sin(-40^\circ)$, when used in the dispersion relation (2), yield the value y_{\min} according to

$$y_{\min} = \frac{1}{K-u^2} \left[u + \sqrt{K [1+(s/a)^2] - u^2 (s/a)^2} \right] \quad (9)$$

This value of y , in turn, used with K , u and the specified maximum frequency-rate of scan (1) in eq. (5), yields the frequency limit ν_{\min} . The values of y_{\max} , occurring for $x = 0$ (corresponding to $\theta = 0$) in this style of scan, determine a relative bandwidth $2(y_{\max} - y_{\min})/(y_{\max} + y_{\min})$ and thereby determine the upper frequency ν_{\max} and the band center $(\nu_{\max} + \nu_{\min})/2$ with which the points in Fig. 9 are labeled. The figure indicates the portion of the plane for which the frequency-rate of scan specification is realizable if bounded by a parabola. The map shows how the tunable bandwidth can be reduced at the expense of increased operating frequency and increased dielectric constant (hence increased dissipation due to the reduction of conductor dimensions and the contribution of dielectric loss). The accessible portion of the plane of the diagram is limited by the onset of spurious grating lobes starting at the point, in Fig. 8. at which the grating lobe line, $y = 2-x$, intersects the dispersion curve. For $\theta_{\max} = 0$, this occurs at $x = 0$. In this style of scan, a more restrictive limitation, occurring at the other end of the scan range θ_{\min} is that which results from the frequency-rate of scan specification, as represented in Fig. 8 by the requirement that the slope of the dispersion curve at θ_{\min} , must remain above that imposed by eq. (5). The effect of this is indicated by the contour labeled " $d\theta/d\nu \rightarrow \infty$ ". To illustrate the conclusions available from

Fig. 9, we note that for the style of scan represented there, namely $-40^\circ < \theta < 0^\circ$, if ordinary empty rectangular waveguide is used ($K = 1$) the band is limited to lie in the 17 GHz to 40 GHz range, with tunable bandwidth ranging from 49% down to about 25%. (Note that the limit $s/a \rightarrow 0$ may be interpreted in the sense $a \rightarrow \infty$ which, by eq. (2), represents the dispersion characteristic of TEM transmission lines such as stripline.)

Fig. 10 represents for comparison the corresponding diagram showing band center and tunable bandwidth on the K vs. s/a plane, for the alternative style of scan $\theta_{\min} = -\theta_{\max}$, in the case $\theta_{\max} = 20^\circ$. Note, for instance, that the empty-waveguide design $K = 1$ is not accessible at all in this case due to grating lobes. For this case the further information, namely waveguide width a and spacing of radiating slots, is presented on the same K vs. s/a plane, in Fig. 11. The total number of slots, or rather, the total length required of the antenna, is determined simply by the aperture length required to achieve the specified beamwidth, as shown graphically in Fig. 12.

An alternative design style which may be advantageous for some system requirements is the so-called "serpentine" line, illustrated in Fig. 13. An increase in the dispersive effect is achieved by adding line length between elements such that for element spacing s , the length of transmission line between elements is the factor F times s . While increasing dispersion with the objective of reducing the tunable bandwidth requirement, this modification is substantially limited by the instantaneous-bandwidth specification. Nevertheless, a successful compromise is conceivably

achievable; simplicity in manufacture could be achieved by use of stripline with printed-circuit fabrication techniques. The effect of serpentine on the dispersion relation is illustrated in Figs. 13 and 14, showing that the scan-angle boundaries θ_{\min} , θ_{\max} determined by eq. (4), $x/y = \sin \theta$, are displaced by the serpentine effect and required to satisfy

$$x = \frac{1}{F} (y \sin \theta + 1 - F) \quad (10)$$

with corresponding reduction in $y_{\max} - y_{\min}$ and also in $y(d\theta/dy)$, as illustrated in Fig.14. An example of a stripline serpentine line is represented as the contour shown in Fig. 15. In this case, the value of $d\theta/d\nu$ was taken to be 8 mrad per 25 MHz. For 15% bandwidth and a range of K from 1 to 3 the center frequency ranges from 31.76 to 25.88 GHz.

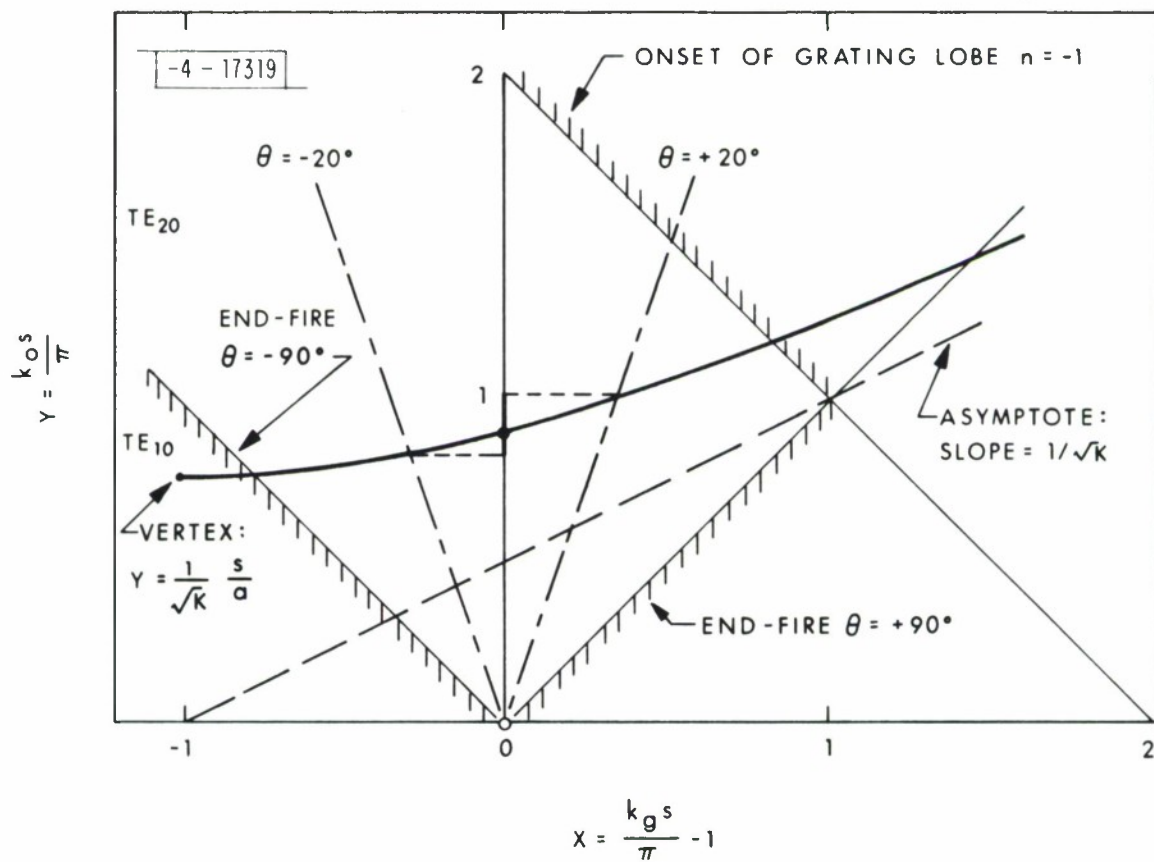


Fig. 8. Frequency scanned antenna dispersion diagram.

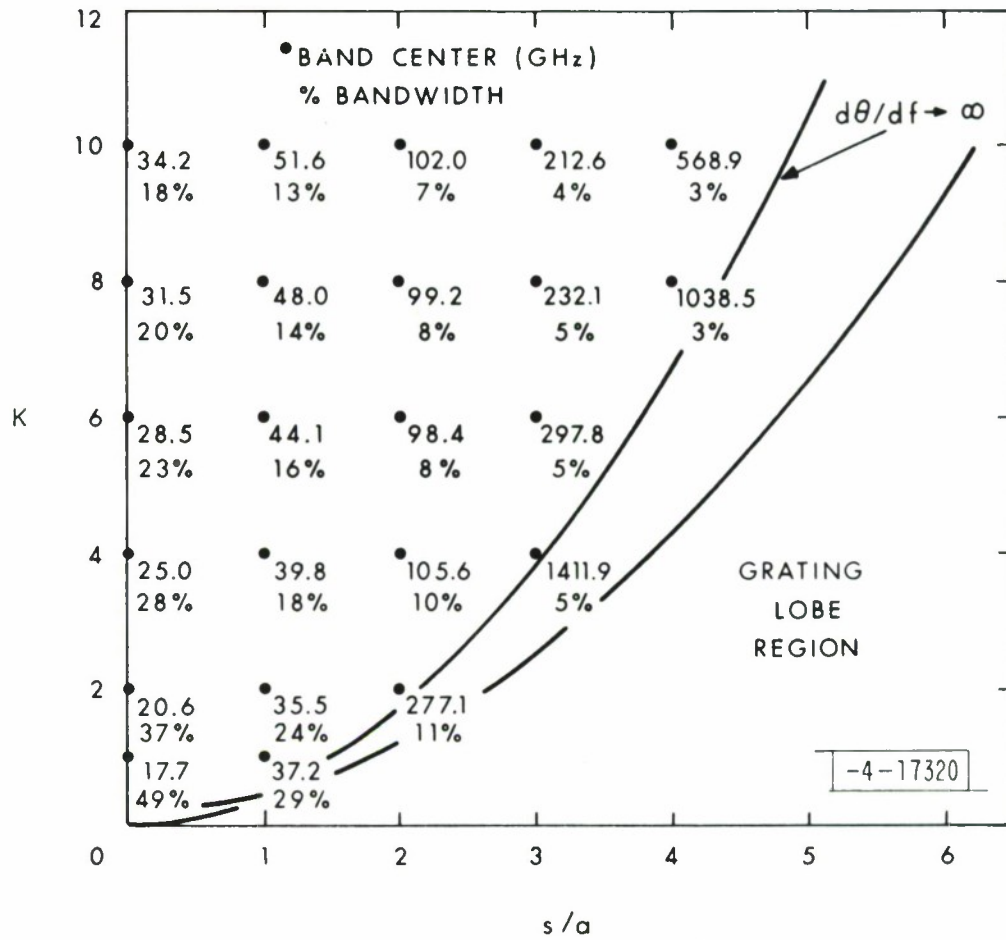


Fig. 9. Bandwidth and center frequency of -40° to 0° scan designs.

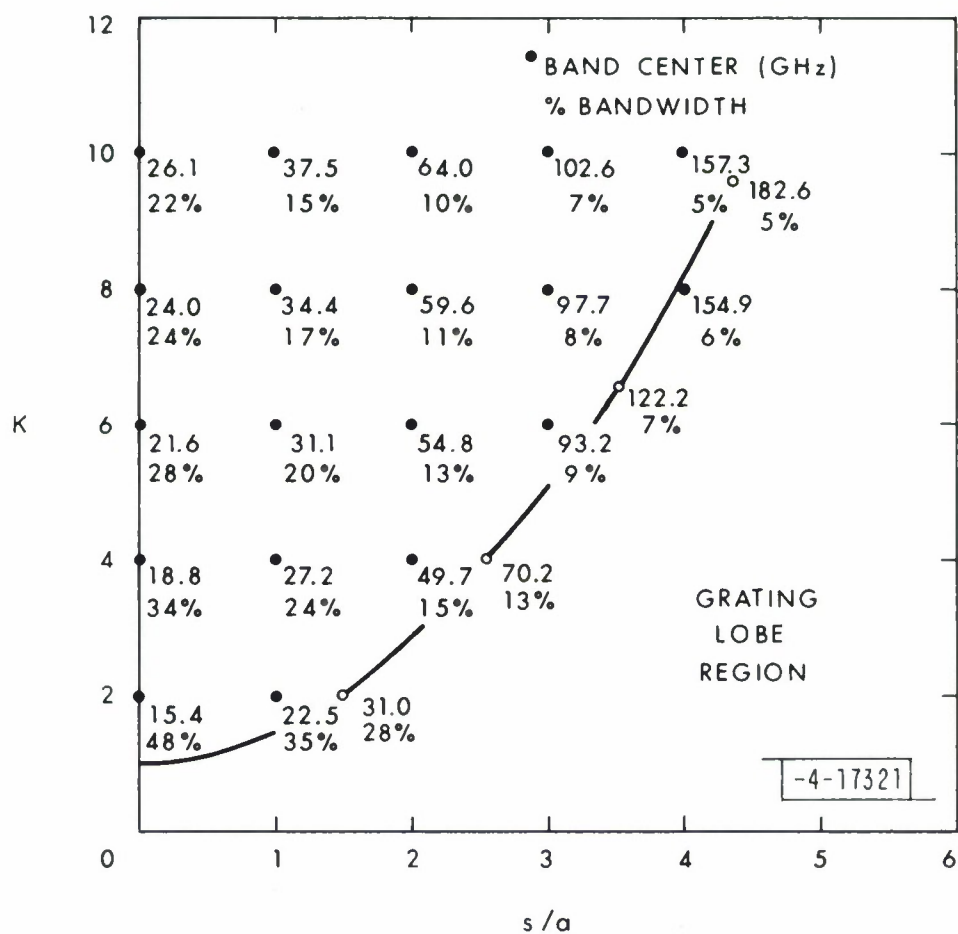


Fig. 10. Bandwidth and center frequency of -20° to $+20^\circ$ scan designs.

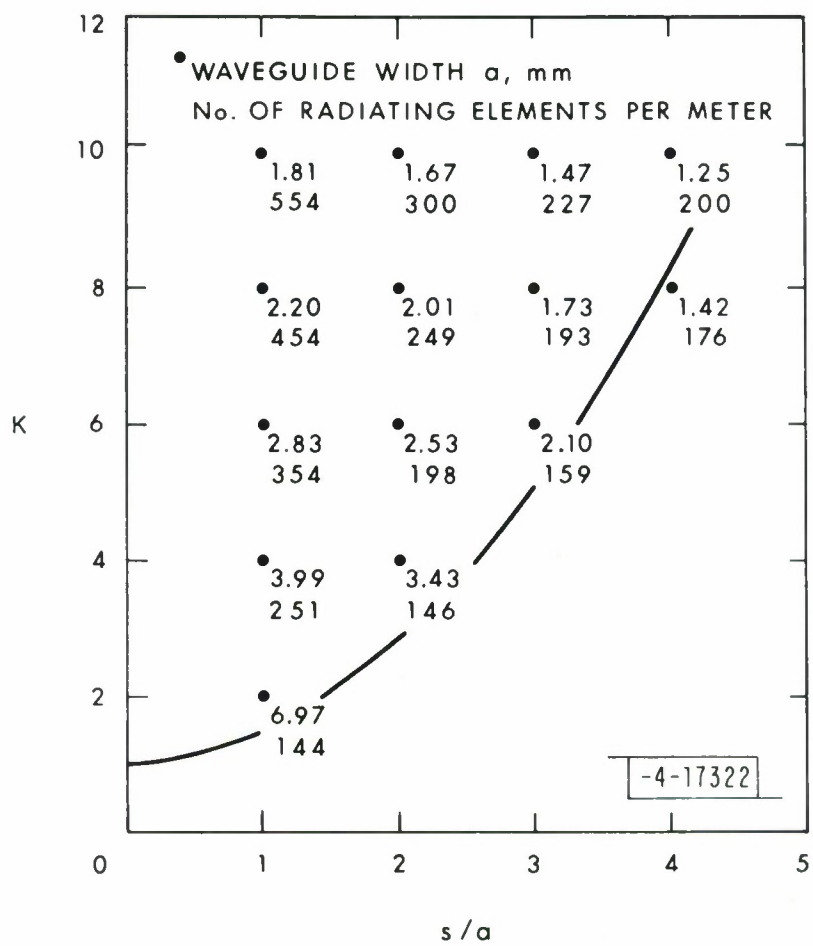


Fig. 11. Waveguide width and number of elements for -20 to +20 scan.

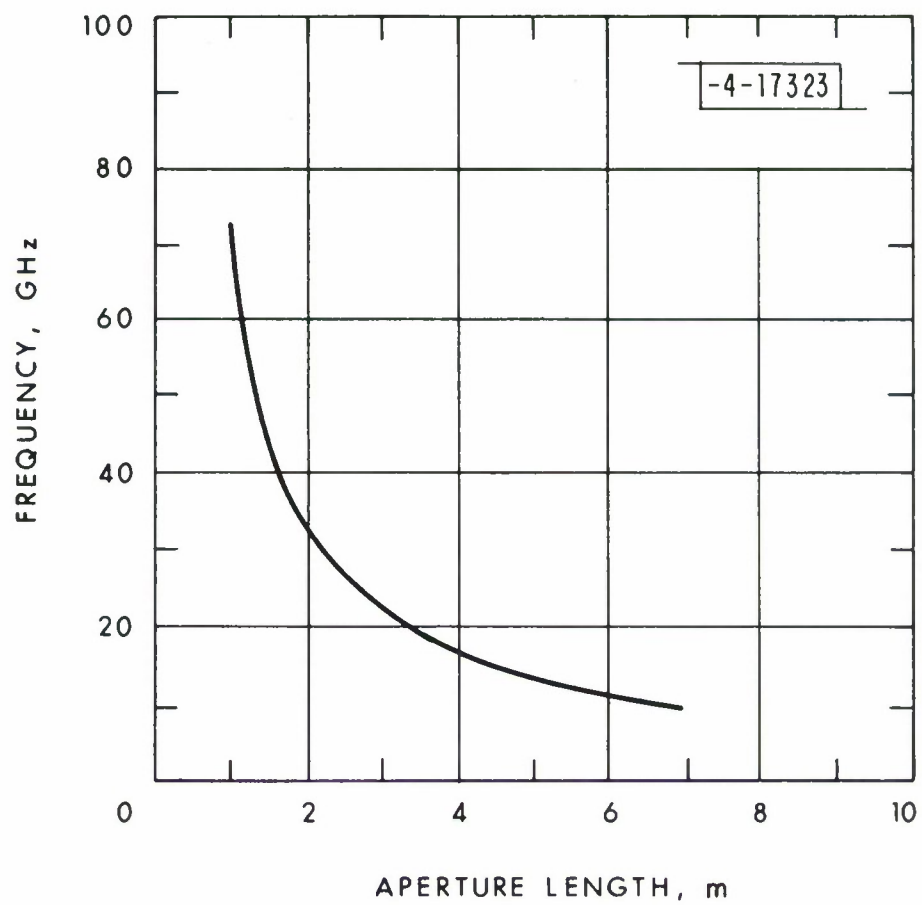


Fig. 12. Aperture length vs. frequency for 4 mrad beamwidth.

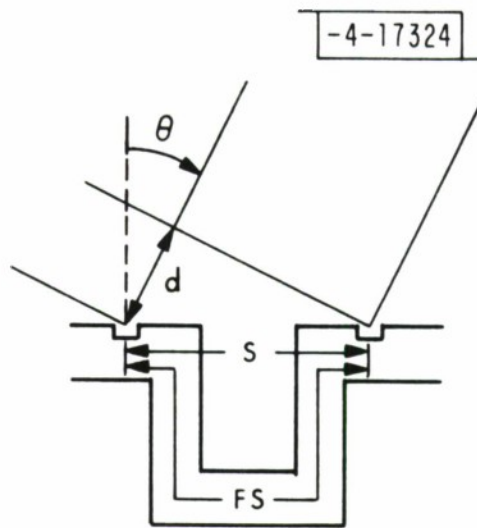


Fig. 13. Serpentine line.

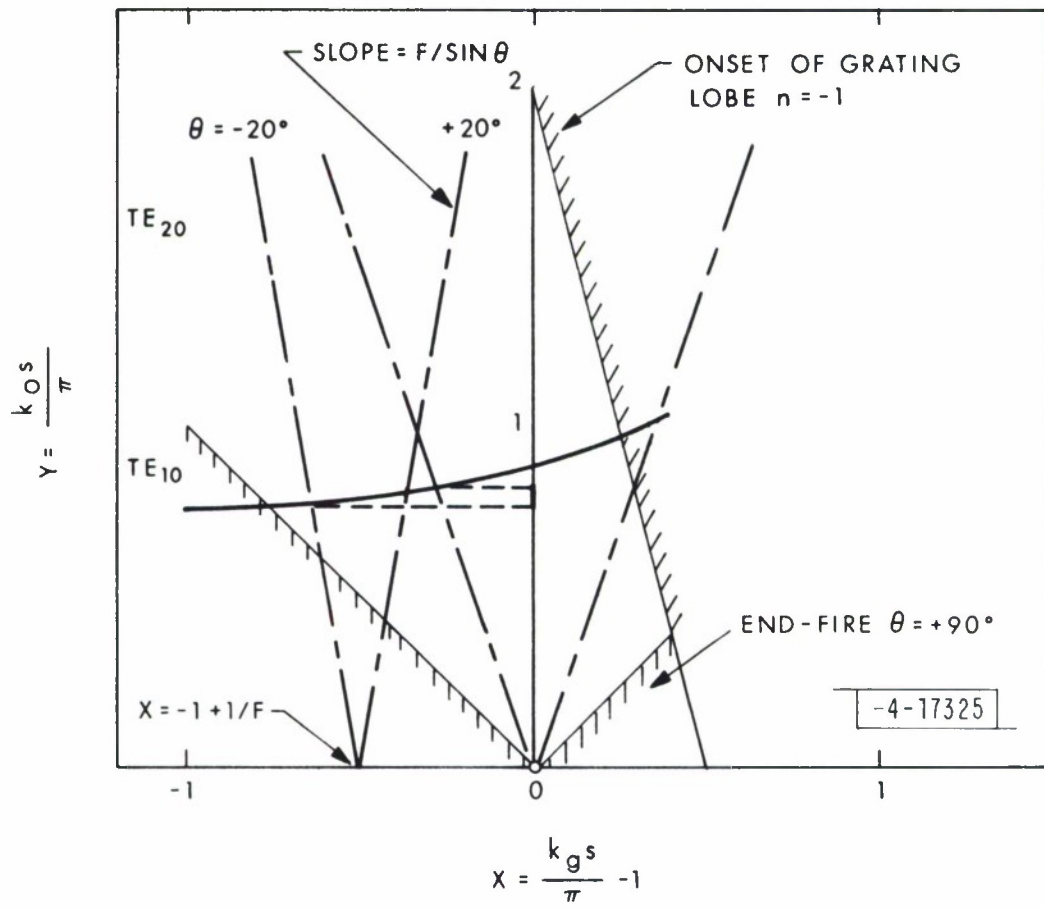


Fig. 14. Serpentine line $F = 2$ dispersion diagram.

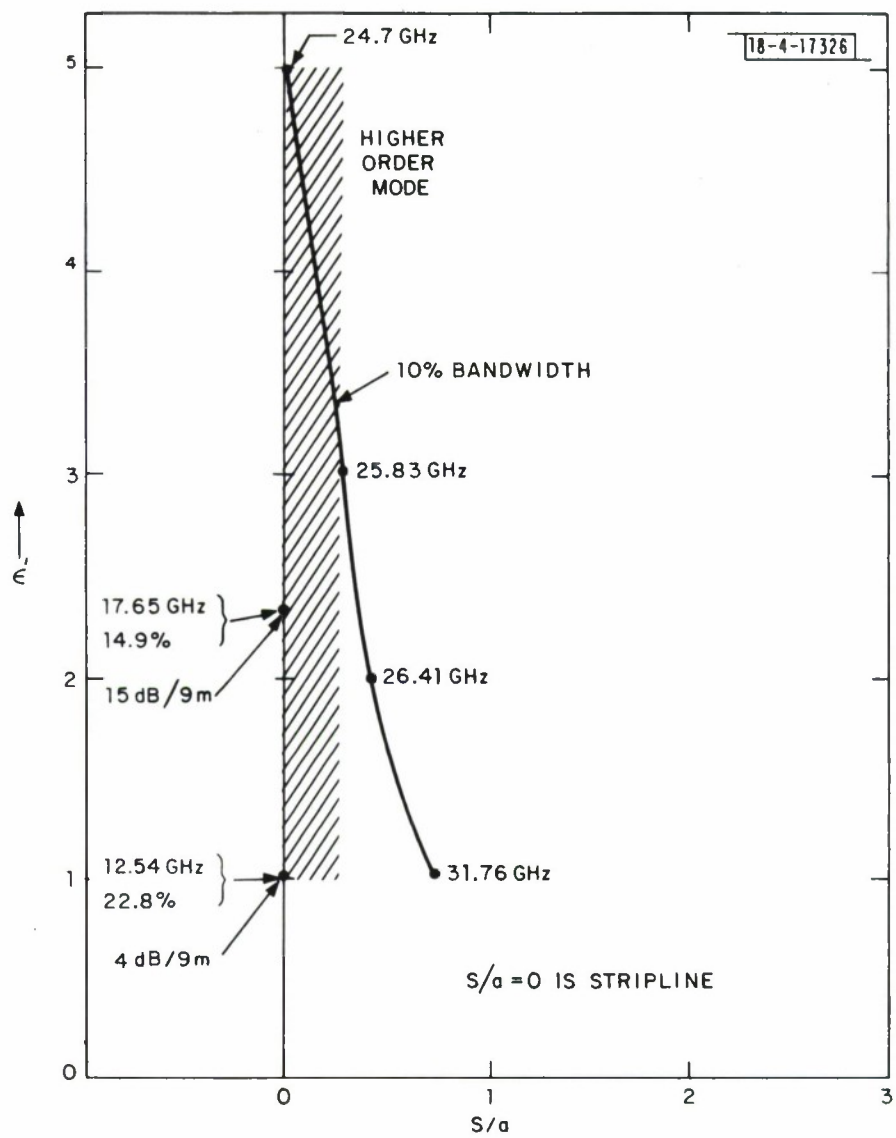


Fig. 15. Bandwidth and center frequency $F = 3$ serpentine line design -20° to $+20^\circ$ scan.

REFERENCES

1. J. L. Hilburn et al., "Frequency Scanned X-band Waveguide Array," IEEE Trans. Antennas Propag. AP-20, 506-509 (1972).
2. H. Jasik, Antenna Engineering Handbook (McGraw-Hill, New York, 1961).
3. A. L. Maffett, "Array Factors with Non-Uniform Spacing Parameter," Trans. IRE, AP-10, 131-136 (1962).
4. A. Ishimaru, "Theory of Unequally-Spaced Arrays," Trans. IRE, AP-10, 691-702 (1962).
5. M. I. Skolnik, J. W. Sherman, and F. C. Ogg, "Statistically Designed Density-Tapered Arrays," Trans. IEEE, PTGAP AP-12, 408-417 (1964).
6. Y. T. Lo, "Random Periodic Arrays," Radio Sci. 3, 425-436 (1968).
7. B. D. Steinberg, "The Peak Sidelobe of the Phased Array Having Randomly Located Elements," IEEE Trans. Antennas Propag. AP-20, 129-136 (1972).

UNCLASSIFIED

SECURITY CLASSIFICATION OF THIS PAGE (When Data Entered)

REPORT DOCUMENTATION PAGE		READ INSTRUCTIONS BEFORE COMPLETING FORM
1. REPORT NUMBER ESD-TR-75-285	2. GOVT ACCESSION NO.	3. RECIPIENT'S CATALOG NUMBER
4. TITLE (and Subtitle) Frequency Scan Antenna Design for RPV Radar Sensors		5. TYPE OF REPORT & PERIOD COVERED Project Report
		6. PERFORMING ORG. REPORT NUMBER Project Report TT-5
7. AUTHOR(s) Willwerth, Francis G. Weiss, Jerald A.		8. CONTRACT OR GRANT NUMBER(s) F19628-76-C-0002
9. PERFORMING ORGANIZATION NAME AND ADDRESS Lincoln Laboratory, M.I.T. P.O. Box 73 Lexington, MA 02173		10. PROGRAM ELEMENT, PROJECT, TASK AREA & WORK UNIT NUMBERS Program Element No. 62702E ARPA Order 2752
11. CONTROLLING OFFICE NAME AND ADDRESS Advanced Research Projects Agency 1400 Wilson Boulevard Arlington, VA 22209		12. REPORT DATE 22 October 1975
		13. NUMBER OF PAGES 44
14. MONITORING AGENCY NAME & ADDRESS (if different from Controlling Office) Electronic Systems Division Hanscom AFB Bedford, MA 02173		15. SECURITY CLASS. (of this report) Unclassified
		15a. DECLASSIFICATION DOWNGRADING SCHEDULE
16. DISTRIBUTION STATEMENT (of this Report) Approved for public release; distribution unlimited.		
17. DISTRIBUTION STATEMENT (of the abstract entered in Block 20, if different from Report)		
18. SUPPLEMENTARY NOTES None		
19. KEY WORDS (Continue on reverse side if necessary and identify by block number) <div style="display: flex; justify-content: space-between;"> <div>HOWLS Program tactical technology</div> <div>frequency scanned arrays RPV radar system</div> </div>		
20. ABSTRACT (Continue on reverse side if necessary and identify by block number) <p>The feasibility of using frequency scanned arrays in a mini-RPV radar system was investigated. A general formulation of the relationships connecting design parameters for frequency scanned arrays was carried out, and a 30% tunable bandwidth array was constructed and tested.</p>		

UNCLASSIFIED

SECURITY CLASSIFICATION OF THIS PAGE (When Data Entered)